Available online at www.sciencedirect.com
SCIENCE DIRECT®
Biochimica et Biophysica Acta 1609 (2003) 183–192
BIOCHIMICA ET BIOPHYSICA ACTA
BBA
www.bba-direct.com

Protons and calcium alter gating of the hyperpolarization-activated cation current (I_h) in rod photoreceptors

Andrew Todd Malcolm[a], Dmitri E. Kourennyi[b], Steven Barnes[c,d,*]

[a] Neuroscience Research Group, University of Calgary, Calgary, Alberta, Canada T2N 4N1
[b] Department of Biomedical Engineering, Case Western Reserve University, Cleveland, OH, USA
[c] Department of Physiology and Biophysics, Dalhousie University, Halifax, Nova Scotia, Canada B3H 4H7
[d] Department of Ophthalmology, Dalhousie University, Halifax, Nova Scotia, Canada B3H 4H7

Received 18 June 2002; received in revised form 25 November 2002; accepted 3 December 2002

Abstract

We investigated the effects of protons and calcium ions on the voltage-dependent gating of the hyperpolarization-activated, nonselective cation channel current, I_h, in rod photoreceptors. I_h is a cesium-sensitive current responsible for the peak-plateau sag during the rod response to bright light. The voltage dependence of I_h activation shifted about 5 mV per pH unit, with external acidification producing positive shifts and alkalinization producing negative shifts. Increasing external [Ca^{2+}] from 3 to 20 mM resulted in a large (~ 17 mV) positive shift in I_h activation. External [Ca^{2+}] (20 mM) blocked pH-induced shifts in activation. Cytoplasmic acidification produced by 25 mM sodium acetate led to a negative shift in inactivation (− 9 mV) and internal alkalinization produced with 20 mM ammonium chloride resulted in a positive shift (+ 6 mV). Surface charge binding and screening theory (Gouy–Chapman–Stern) accounted for the observed shifts in I_h activation, with the best fit achieved when protons and calcium ions were assumed to bind to distinct sites on the membrane. Since light induces changes in the retinal ionic environment, these results permit us to gauge the degree to which rod light responses could be modified via alterations in I_h activation.

Keywords: Surface charge; Light response; Ionic environment; Voltage-dependent gating; Perforated patch; HCN channel

1. Introduction

The well-characterized electrical changes that occur in vertebrate rod photoreceptors during illumination are accompanied by changes in the chemical environment surrounding rods during illumination. Rods in the dark have a membrane potential of about − 40 mV and hyperpolarize in response to light. If strong enough, this hyperpolarization activates a voltage-dependent nonselective monovalent cation current, I_h. The resultant depolarizing roll-back (''peak-plateau sag'') is the primary mechanism shaping the rod voltage response to bright light [2,3]. At the same time, the extracellular space surrounding rods alkalinizes during illumination [10,11,39,41,54]. This change in pH_o is thought to arise from a decrease in rod metabolism. An increase in $[Ca^{2+}]_o$ also accompanies illumination [17,21,34,55,56]. Several factors appear to contribute to the $[Ca^{2+}]$ changes: (1) reduced Ca^{2+} influx through cyclic nucleotide gated (CNG) channels, (2) continued extrusion of Ca^{2+} via Na/Ca/K exchanger, (3) increased extracellular volume and (4) calcium pumps (or exchangers) in retinal pigment epithelial cells [17,34].

Extracellular Ca^{2+} and pH are known to alter the gating of voltage-dependent ion channels. For example, shifts in the voltage-dependent activation of L-type calcium channels, Kx channels, Ca-activated Cl channels and h channels in photoreceptors have been observed upon changing $[Ca^{2+}]_o$ and/or pH_o [6,7,32,43,51,52]. For each voltage-dependent ion channel, the observed effects have been qualitatively similar—increasing $[Ca^{2+}]_o$ or decreasing pH_o results in a shift of the activation curves to more depolarized levels, while decreasing $[Ca^{2+}]_o$ or increasing pH_o results in hyperpolarizing shifts of the activation curves. Ca^{2+} and pH are thought to bring about these gating changes via alterations of the membrane surface charge.

* Corresponding author. Department of Physiology and Biophysics, Dalhousie University, Halifax, Nova Scotia, Canada B3H 4H7. Tel.: +1-902-494-3367; fax: +1-902-494-6309.
E-mail address: sbarnes@is.dal.ca (S. Barnes).

0005-2736/02/$ - see front matter © 2002 Elsevier Science B.V. All rights reserved.
doi:10.1016/S0005-2736(02)00687-9

Previous studies have suggested that cations, such as H^+ and Ca^{2+}, alter the membrane surface charge by screening fixed membrane charges (Gouy–Chapman theory), binding to these charges (Gouy–Chapman–Stern theory), or through a combination of both mechanisms [13,18,23,24,26,30,31,37,42,50]. This work examines how pH_o, $[Ca^{2+}]_o$ and pH_i affect I_h and whether or not the alterations are consistent with surface charge theory.

Recent elaboration of the molecular structure of the channels underlying I_h (HCN channels) in several species offers insight into the mechanisms with which these channels gate [19,27,35,45]. Although HCN channels enter conductive states with increasing membrane hyperpolarization, we now know that the putative voltage-sensing S4 transmembrane spanning helix of HCN channels is similar to the S4 region of channels activated by depolarization (positively charged residues at approximately every third position). The fact that HCN channels share this region with depolarization-activated channels leads to speculation that, for HCN channels, either the S4 region is not involved in gating, the coupling mechanism between S4 movement and channel opening is reversed, or that other gating schemes predominate, e.g. transitions to conducting states in HCN channels induced by hyperpolarization reflect transitions from inactivated to activated states (discussed in Ref. [46]). Should HCN channel gating modifications brought about by protons and calcium be remarkably different than those seen in depolarization-activated channels, clues about the mechanism by which hyperpolarization opens the channels could be provided.

2. Materials and methods

Larval tiger salamanders, *Ambystoma tigrinum* (Kons Scientific Supply, Germantown, WI), kept at 6–8 °C in a refrigerator under an 8:16-h light/dark cycle, were killed by decapitation. After enucleation, the cornea and lens of the eye were removed, and the retina was peeled out in standard bath solution. The rods were mechanically isolated with gentle trituration using a fire-polished Pasteur pipette. The cells were then plated in 0.5-ml wells formed with Sylgard® 182 in plastic petri dishes. Recordings were made at room temperature (21–22 °C) from light-adapted rods exposed to constant illumination in a Nikon Diaphot microscope.

The standard bath solution contained (in mM): 90 NaCl, 2.5 KCl, 3 $CaCl_2$, 8 D-glucose and 10 HEPES, and was adjusted to pH 7.6 with NaOH. Test pH_o solutions contained the same components as the standard bath solution except the amount of NaOH added was changed to give a final pH near 6.0, 7.0, 7.3, 7.9 or 8.2. Test $[Ca^{2+}]_o$ solutions contained the same components as the standard bath solution except the amount of $CaCl_2$ was altered from 3 mM (control) to affect a final $[Ca^{2+}]_o$ of 0.5, 10 or 20 mM. For internal alkalinization or acidification, ammonium chloride (NH_4Cl) and sodium acetate (NaAcetate) solutions had equimolar concentrations of NaCl replaced with 20 mM NH_4Cl or 25 mM NaAcetate, respectively. Test solutions were superfused over the cells for 1–2 min, and washed off for 2–5 min. The electrode filling solution consisted of (in mM): 100 KCl, 10 HEPES, 3.5 $MgCl_2$, 1.5 Na_2ATP and 1 EGTA, and was adjusted to pH 7.2 with KOH. All chemicals were obtained from Sigma Chemical Company (St. Louis, MO). Patch pipettes were pulled from soft, thin-walled hematocrit glass tubes (VWR Scientific, West Chester, PA) in two steps on a vertical puller (Kopf model 730, Tujunga, CA). When filled with this solution, the pipettes had resistances between 5 and 10 MΩ. Currents were measured using the perforated patch whole-cell voltage-clamp method [29]. The tip of the patch pipette was filled with solution and then the pipette was back-filled with nystatin-containing solution (150 μg/ml). The time required to gain access to the cell, judged from the development and decrease in time constant of capacitance currents, varied from 1 to 10 min. The whole-cell currents were recorded using an Axopatch-200 or Axopatch-1B amplifier (Axon Instruments, Burlington, CA) and Basic-Fastlab software (Indec Systems, Sunnyvale, CA).

The range of voltages over which I_h activates was assessed with a specific voltage-clamp paradigm. No chemical agents were added to block other conductances. Instead, −80 mV was chosen as a test potential at which I_h could be isolated. Over the range of voltages tested (e.g. −40 to −110 mV), I_{Kx} is the major contaminant but its contributions to whole cell current were removed by evoking I_h tails at −80 mV (see Fig. 1), a potential that is close to the reversal potential for I_{Kx} under the conditions tested here (−79 mV, Ref. [8]). Tail currents were fit with single exponential functions and current magnitude was measured from the exponential fit *extrapolated* to the beginning of the −80 mV step. Activation curves were fit with the Boltzmann equation:

$$\frac{I_{h,V} - I_{h,-110}}{I_{h,max}} = \frac{1}{1 + e^{\frac{V - V_{1/2}}{z}}}, \quad (1)$$

where $I_{h,V}$ and $I_{h,-110}$ are the extrapolated amplitudes of I_h tail current obtained after conditioning steps to V mV and after the most hyperpolarized conditioning step (−110 mV in most cases); $I_{h,max}$ is the extrapolated tail current envelope amplitude (spanning the range from −40 to −110 mV, see Fig. 1); $V_{1/2}$ is the half-activation potential; and z is the slope factor.

The activation parameters at each test condition (pH_o, $[Ca^{2+}]_o$ and pH_i) were estimated with respect to linear interpolation between control (before) and wash (after) values. Statistical data are presented as means ± S.E.M. and statistical significance was estimated using the paired two-tailed Student's *t*-test. Significance was considered at $P < 0.05$.

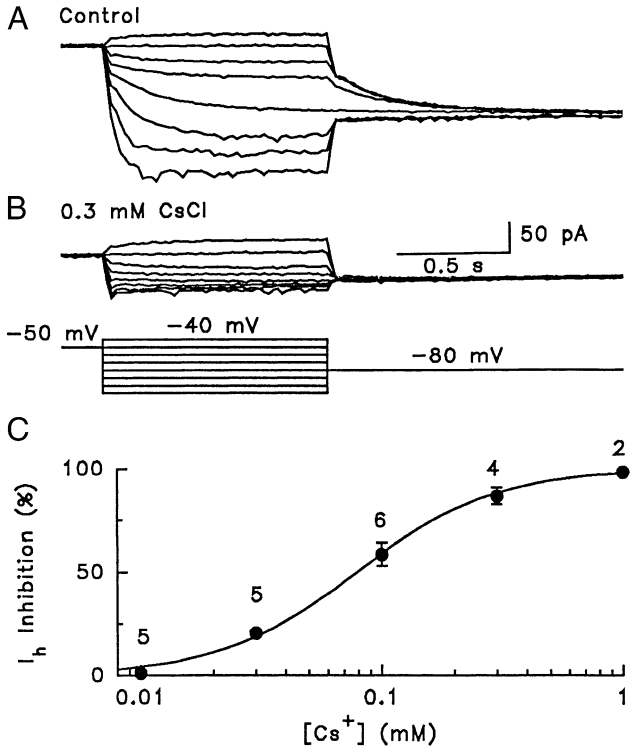

Fig. 1. Isolation of I_h at −80 mV. (A) Voltage clamp recording of I_h from a rod photoreceptor. The membrane potential was held at −50 mV and shifted for 1 s to conditioning steps ranging from −40 to −110 mV with 10-mV increments to evoke tail currents at −80 mV. Arrows indicate the tail current envelope encompassing the full activation range of I_h. (B) CsCl (0.3 mM) blocked the tail currents and most of the inward current that developed during the conditioning steps. The current gated by the conditioning steps resembles I_{Kx}, which reverses near −80 mV under the conditions of this experiment, and is therefore not present at −80 mV (7). (C) Inhibition of I_h by CsCl was measured over a range of 0.01 to 1 mM CsCl. The data were fit by a cooperative binding function having K_D=79.6 μM and Hill coefficient of 1.47. The numbers above each data point indicate the number of observations at that concentration.

NH_4Cl and NaAcetate were utilized to increase or decrease pH_i of the rods (see Refs. [44,48,49]). A superfusion protocol similar to that utilized by Takahashi and colleagues was used in the present study so that their measurements could be used as approximations for expected pH_i changes in rod photoreceptors.

We determined the degree to which the effects of pH_o and $[Ca^{2+}]_o$ on I_h gating are consistent with surface charge theory. The Grahame equation [20,36] describes the relationship between the density of membrane surface charges, concentration of ions in the medium, and the surface potential:

$$\sigma^2 G^2 = \sum_{i=1}^{n} C_i\left(e^{-\frac{z_i F \psi_o}{RT}} - 1\right), \tag{2}$$

where σ is the surface charge density in $e^-/Å^2$, G is a constant with value of 270 $Å^2\ e^{-1}\ M^{1/2}$, RT/F=25.3 mV at 22 °C, C_i is the concentration of the ith ion species in the bulk solution, z_i is its valence, and ψ_o is the surface potential in mV.

Assuming that H^+ and Ca^{2+} ions bind to common negative surface charges [18], the apparent charge density is reduced and now the relationship between the apparent and true negative surface charge density is [31]:

$$\sigma_a = \frac{\sigma}{1 + K_H[H^+]^* + K_{Ca}[Ca^{2+}]^*}, \tag{3}$$

where K_H and K_{Ca} are the apparent association constants for H^+ and Ca^{2+} ions, respectively.

Assuming that H^+ and Ca^{2+} bind to different surface sites, the relationship between the apparent and true negative surface charge density is [9,24]:

$$\sigma_a = \frac{\sigma_1}{1 + K_H[H^+]^*} + \frac{\sigma_2}{1 + K_{Ca}[Ca^{2+}]^*}, \tag{4}$$

where σ_1 and σ_2 are true surface densities of binding sites for H^+ and Ca^{2+}, respectively.

In Eqs. (3) and (4), $[H^+]^*$ and $[Ca^{2+}]^*$ are the surface concentrations of H^+ and Ca^{2+}, respectively, which are related to bulk concentrations $[H^+]$ and $[Ca^{2+}]$ by the following relations:

$$[H^+]^* = [H^+]\exp(-\psi_o e/kT),$$

$$[Ca^{2+}]^* = [Ca^{2+}]\exp(-2\psi_o e/kT). \tag{5}$$

For the fixed charge densities in a range of 25 to 6400 $Å^2$, Eqs. (2) and (5) were numerically solved together with Eq. (3) or Eq. (4) by varying K_H and K_{Ca}. Experimental shifts in I_h activation were fitted with calculated changes in ψ_o.

3. Results

3.1. Tail current measurement protocol isolates I_h

This investigation required a reliable means for isolating I_h. A voltage clamp recording paradigm used to isolate I_h is presented in Fig. 1A. This record is from a rod photoreceptor that was voltage clamped at a holding potential of −50 mV, and then stepped for 1 s to a series of conditioning steps, each decremented by 10 mV (ranging from −40 to −110 mV), before a test step to −80 mV was applied to generate tail currents.

The conditioning steps evoke two superimposed currents, I_h and I_{Kx}, but the test step to −80 allows I_h to be isolated in the tails (see Materials and methods). To confirm that this protocol effectively isolates I_h in the tail currents, CsCl was superfused over the cells since external Cs^+ is a known blocker of I_h but not of I_{Kx} [8]. Fig. 1B shows that application of 0.3 mM CsCl effectively blocked the tail

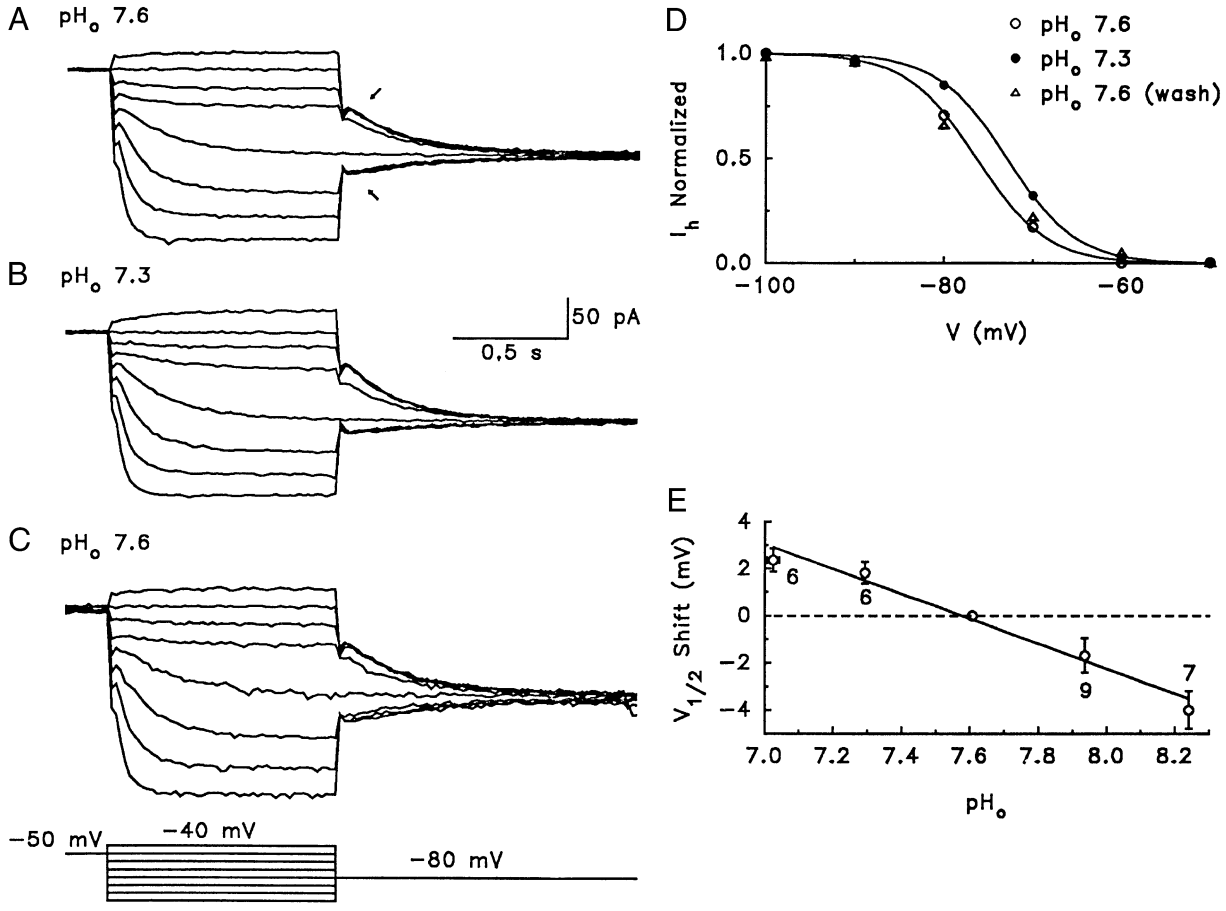

Fig. 2. External acidification shifts I_h activation to positive potentials. (A) Voltage clamp recording of I_h at control pH_o 7.6, at test pH_o 7.3 and upon wash. (B) Boltzmann equation fits of the activation curve for I_h at pH_o 7.6 (control and wash, open symbols) and at pH_o 7.3. (C) A plot of $\Delta V_{1/2}$ vs. pH_o. The number of cells studied is shown near each symbol. The solid line represents a linear regression fit described by $\Delta V_{1/2} = 39.8$ mV − 5.25 mV/pH* (pH unit).

currents evoked at − 80 mV and most of the inward current that developed during the conditioning steps. The current remaining is I_{Kx}, as described previously [8].

Cs^+ blocked I_h in a dose–response manner (Fig. 1C). Block of I_h was calculated by comparing the tail current envelope in the test solution to that in control (indicated by arrows in Fig. 1A). The dose dependence was fitted assuming a cooperative interaction between Cs^+ and h channels that gave values for K_D and n (Hill coefficient) of 79.6 μM and 1.47, respectively.

3.2. External pH (pH_o) affects I_h gating

An example of how changing pH_o affects I_h is shown in Fig. 2. The current traces were obtained from a rod that was initially exposed to control solution (pH_o 7.6; Fig. 2A), then to a more acidic solution (pH_o 7.3; Fig. 2B) for 1 min, and finally washed with control solution (Fig. 2C). The equal-sized tail current envelopes obtained in this cell show that the maximum magnitude of I_h was not affected by changing pH_o, but that its activation was shifted in the positive direction. In this cell a +3.6 mV shift in $V_{1/2}$ was observed (Fig. 2D).

This type of analysis was conducted for each test pH_o solution, and shifts in $V_{1/2}$ ($\Delta V_{1/2}$) obtained from different cells were combined and averaged. The resulting data are plotted against pH_o relative to the value $\Delta V_{1/2} = 0$ defined for control pH_o 7.6 (Fig. 2E). The linear fit yielded a positive shift of 5.25 mV per pH unit acidification. In addition to changes in the activation curve midpoint, pH_o

Table 1
Effects of pH_o on activation parameters of I_h

pH_o	$\Delta V_{1/2}$ (mV)	$I_{h,max}$ (normalized)	Z (normalized)	τ (normalized)
6.98–7.07 ($n=6$)	2.37 ± 0.50, $0.001 < P < 0.01$	0.92 ± 0.05, $0.2 < P < 0.3$	0.88 ± 0.11, $0.3 < P < 0.4$	1.02 ± 0.06, $0.7 < P < 0.8$
7.26–7.32 ($n=6$)	1.83 ± 0.04, $0.01 < P < 0.02$	0.96 ± 0.02, $0.8 < P < 0.9$	0.99 ± 0.06, $0.5 < P < 0.6$	1.01 ± 0.03, $0.7 < P < 0.8$
7.92–7.95 ($n=9$)	− 1.69 ± 0.7, $0.02 < P < 0.05$	1.09 ± 0.02, $0.001 < P < 0.01$	1.04 ± 0.07, $0.5 < P < 0.6$	0.95 ± 0.03, $0.5 < P < 0.6$
8.20–8.31 ($n=7$)	− 4.00 ± 0.8, $0.001 < P < 0.01$	1.27 ± 0.11, $0.02 < P < 0.05$	1.37 ± 0.11, $0.01 < P < 0.02$	0.86 ± 0.05, $0.02 < P < 0.05$

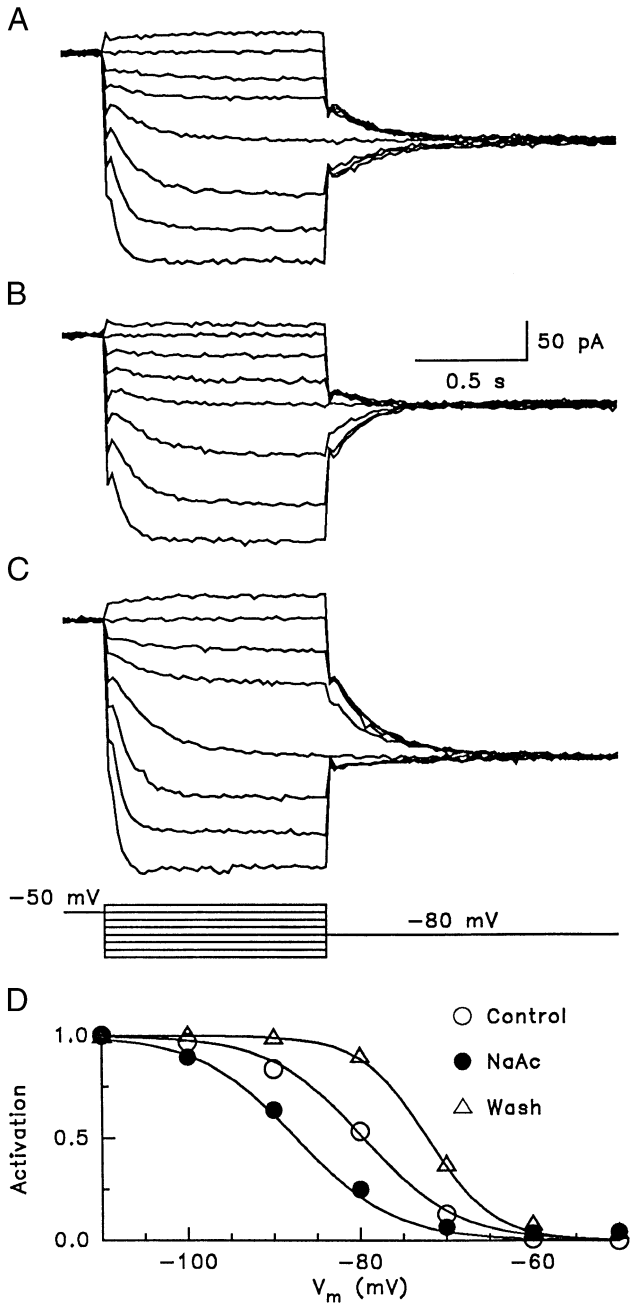

Fig. 3. Decreasing internal pH shifts I_h activation to more negative potentials. Voltage clamp recording of I_h in control (A), after superfusion of 25 mM NaAcetate (B) and wash (C). An estimated decrease in pH_i of 0.6 pH units would be expected with this treatment (Takahashi et al. [49]). (D) Activation curves for I_h from the cell illustrated. Note the overshot positive shift during wash.

induced small changes in the amplitude of I_h, the slope factor of the activation curve, and the time constant for current activation at −80 mV. The values for $\Delta V_{1/2}$ and the normalized changes in other activation parameters (maximum current amplitude, slope factor, time constant) during the pH_o changes, including their significance levels, are summarized for all cells studied in Table 1. Although current amplitude increased with increasing pH, and the time constant for activation at −80 mV became shorter as pH increased, few of the activation parameter change were statistically significant.

3.3. Changes in pH_i alter I_h gating

To make the interior of the photoreceptor more acidic, 25 mM NaAcetate was superfused for 2 min over the cells. Using results obtained in retinal horizontal cells [49], an estimated decrease in pH_i of 0.6 pH units would be expected. An example of how NaAcetate affected I_h is shown in Fig. 3. During application of NaAcetate, a change in the tail currents is apparent. The tail current evoked after the −80 mV conditioning step is shifted from the middle of the tail current envelope to the upper boundary, indicating an activation shift in the hyperpolarizing direction. The speed with which the tail currents developed (τ) also changed during and after the NaAcetate superfusion, an effect that can be explained by pH_i-induced shifts of the activation curve provided that the τ vs. voltage curve shifts the same amount as the activation curve. Tail current derived activation curves show a −9 mV shift after NaAcetate superfusion and a 7 mV overshoot positive to control upon wash (Fig. 3D). Such a large overshoot during washout of NaAcetate may be caused by the increase in pH_i expected to accompany the rapid loss of protons from the cytoplasm as protonated acetate molecules leave the cell in this nominally bicarbonate-free system. In four cells studied, NaAcetate superfusion shifted activation by -9 ± 2.3 mV, reduced I_h magnitude to $88 \pm 11\%$ of control, increased slope factor by $121 \pm 31\%$, and shortened τ to $76 \pm 11\%$ of

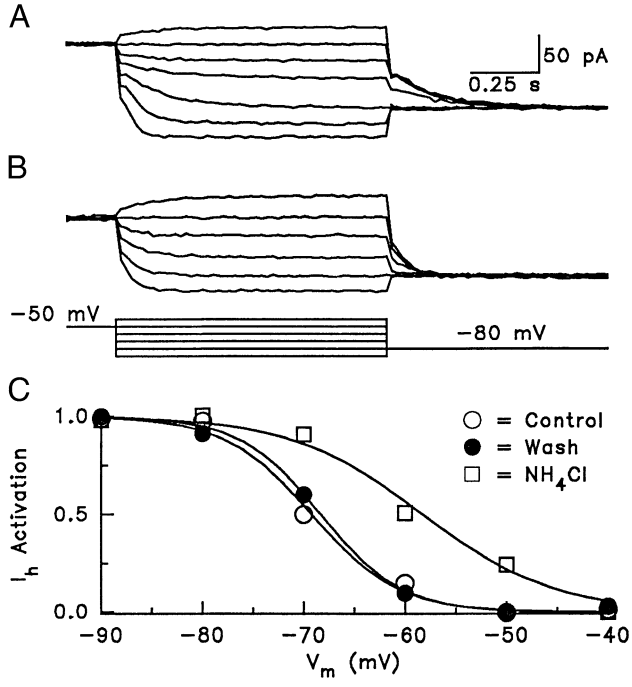

Fig. 4. Voltage clamp recording of I_h in control (A) and after superfusion of 20 mM NH_4Cl (B). (C) Activation curves for I_h from the cell illustrated.

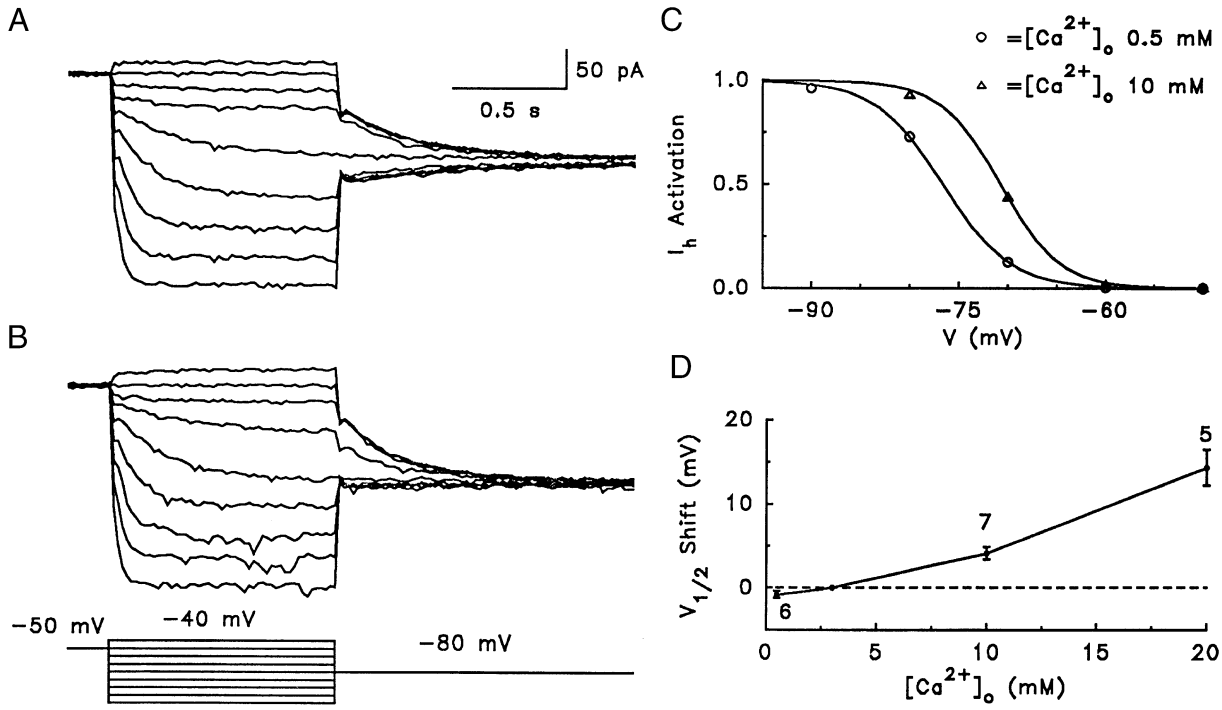

Fig. 5. External calcium shifts I_h activation. Voltage clamp recording of I_h with $[Ca^{2+}]_o$ of 0.5 (A) and 10 mM (B). (C) Activation curves for I_h from the cell illustrated in (A) and (B) fitted with the Boltzmann function. (D) $\Delta V_{1/2}$ vs. $[Ca^{2+}]_o$. The number of cells studied is shown near each symbol.

control values. Only the changes to $V_{1/2}$ were statistically significant ($P<0.05$).

Internal pH was increased by 2-min applications of 20 mM NH_4Cl, which were expected to produce increases in pH_i of between 0.2 and 0.5 pH unit [44,49]. An example of how NH_4Cl affected I_h is shown in Fig. 4. The tail current elicited after the −70 mV conditioning step was displaced during NH_4Cl application towards the tail currents that represent fully activated I_h, indicating that the activation range of I_h was shifted to more positive potentials. A change in the time constant of the tail current envelope was also observed during NH_4Cl application, which can again be explained by a pH_i-induced shift of τ. A +7 mV shift in activation is seen in the tail current derived activation curves (Fig. 4C). The values for $\Delta V_{1/2}$ and normalized changes in other activation parameters during changes in pH_i can be summarized as follows for five cells tested: $\Delta V_{1/2}$ shifted positive by 5.8 ± 1.3 mV, current magnitude was reduced to 76 ± 15% of control, the slope factor increased by 134 ± 15%, and the activation time constant was shortened to 84 ± 7% of control. Only the shift in $\Delta V_{1/2}$ was statistically significant ($P<0.02$).

3.4. Changes in external calcium shift I_h gating

Considered within the established framework of surface charge effects, our pH_o results suggest that surface potential may be altered by protons. Next the effect of varying $[Ca^{2+}]_o$ on I_h activation was studied. An example of how $[Ca^{2+}]_o$ affected I_h is shown in Fig. 5. As $[Ca^{2+}]_o$ was increased from 0.5 to 10 mM, a shift in I_h activation in the depolarizing direction was apparent in the tail currents. For example, the tail current evoked after the −80 mV conditioning step in 10 mM Ca^{2+}_o is nearer the tail currents representing fully activated I_h (Fig. 5B) than it was in 0.5 mM Ca^{2+}_o (Fig. 5A). The Ca^{2+} sensitivity of gating is depicted in the tail current-derived activation curves (Fig. 5C).

Values for $\Delta V_{1/2}$ obtained at $[Ca^{2+}]_o$ 0.5, 10, and 20 mM from different cells were combined and averaged. The resulting data were plotted against $[Ca^{2+}]_o$ relative to the value $\Delta V_{1/2}=0$ defined at 3 mM $[Ca^{2+}]_o$ (Fig. 5D). The values for $\Delta V_{1/2}$ and relative changes in other activation parameters during changes in $[Ca^{2+}]_o$ are summarized in Table 2.

Table 2
Effects of $[Ca^{2+}]_o$ on activation parameters of I_h

$[Ca^{2+}]_o$	$\Delta V_{1/2}$ (mV)	$I_{h,max}$ (normalized)	Z (normalized)	τ (normalized)
0.5 mM ($n=6$)	−0.8 ± 0.4, $0.1<P<0.2$	1.07 ± 0.04, $0.1<P<0.2$	1.15 ± 0.11, $0.2<P<0.3$	0.91 ± 0.04, $0.05<P<0.1$
10 mM ($n=7$)	4.2 ± 0.7, $P<0.001$	0.96 ± 0.04, $0.1<P<0.2$	0.91 ± 0.12, $0.4<P<0.5$	1.12 ± 0.08, $0.1<P<0.2$
20 mM ($n=5$)	14.4 ± 2.2, $0.001<P<0.01$	0.90 ± 0.05, $0.1<P<0.2$	0.62 ± 0.15, $0.05<P<0.1$	0.82 ± 0.05, $0.001<P<0.01$

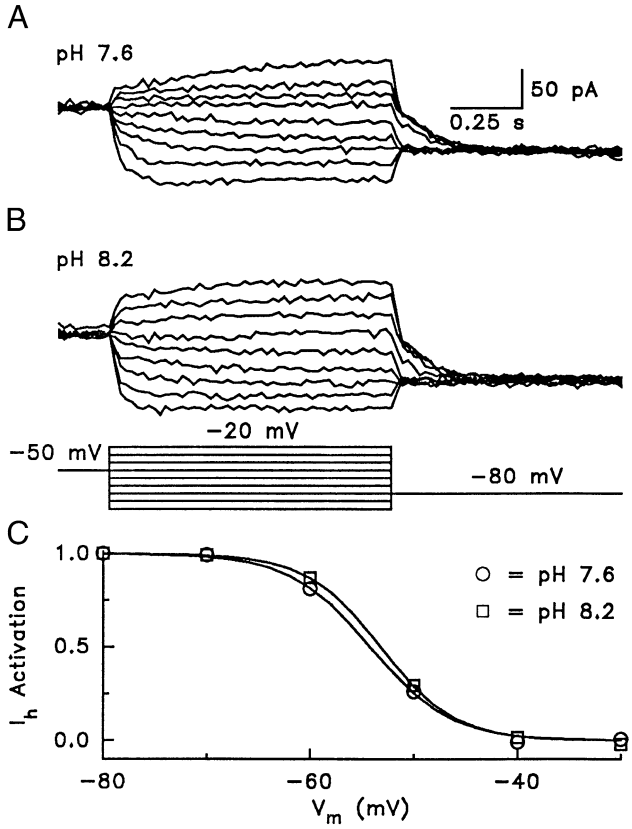

Fig. 6. High $[Ca^{2+}]_o$ eliminates proton-induced gating shifts. (A) Voltage clamp recordings of I_h at pH_o 7.6 and 8.2 while $[Ca^{2+}]_o$ remained at 20 mM. (B) I_h activation curves fitted with Boltzmann function.

3.5. Protons and calcium do not act independently

Qualitatively, the above results appear to be consistent with the hypothesis that pH_o and $[Ca^{2+}]_o$ can alter I_h activation via modifications of the membrane surface potential. If protons and Ca^{2+} bind to similar negative sites, the pH_o-induced shift should be abolished in high $[Ca^{2+}]_o$ and, likewise, a great reduction in Ca^{2+}-induced shift should occur in low pH_o. In contrast, if these ions bind to different negative sites, activation shifts would be expected in both cases.

To determine whether the changes in activation induced by pH_o are affected by $[Ca^{2+}]_o$, pH_o-induced changes in I_h activation were measured in 20 mM $[Ca^{2+}]_o$. Since high calcium produced a large positive shift in $V_{1/2}$, the conditioning steps in many of these experiments were initiated at -20 mV in order to measure full I_h activation. An example of how elevated $[Ca^{2+}]_o$ affected pH-induced shifts is shown in Fig. 6. Tail current-derived activation curves were not affected much by an alkalinization from pH_o 7.6 to pH_o 8.2 in 20 mM $[Ca^{2+}]_o$ (Fig. 6), and these reflected an insignificant -0.9 ± 1.2 mV shift in $V_{1/2}$ in six cells. Other activation parameters (maximum current amplitude, $103 \pm 4\%$; slope factor, $130 \pm 19\%$; and time constant, $106 \pm 9\%$) showed no significant changes as well. Acidification from pH_o 7.6 to pH_o 7.0 in elevated $[Ca^{2+}]_o$ also failed to affect I_h activation ($\Delta V_{1/2}$, 0.0 ± 1.2 mV; maximum current amplitude, $104 \pm 3\%$; slope factor, $124 \pm 20\%$; and time constant, $102 \pm 8\%$). No significant shifts in I_h activation parameters were observed during changes to pH_o 7.0 or 8.2 from pH_o 7.6.

The above experiments demonstrated that pH_o-induced shifts in activation are suppressed by high calcium. In order to observe how pH_o affects calcium-induced shifts, experiments were carried out in pH_o 6.0 while $[Ca^{2+}]_o$ was changed. Under these conditions, changing $[Ca^{2+}]_o$ from 0.5 to 20 mM produced a positive shift in $V_{1/2}$ of about 10 mV in the cell shown (Fig. 7), although cell stability was compromised. In two cells, average values for $\Delta V_{1/2}$ were 10.4 ± 0.1 mV, which were significant at the $P < 0.01$ level. Owing to this large shift, normalized values of time constant for activation at -80 mV were also significant ($P < 0.01$) at $85 \pm 1\%$. The other activation parameters (maximum current amplitude, $98 \pm 1\%$; and slope factor, $99 \pm 3\%$) failed to reach significance when compared to control.

Surface potential theory was utilized to aid in the interpretation of the data. Estimates of surface charge density and binding constants in the surface potential equations (see Materials and methods) were determined assuming that shifts in I_h activation were due to pH_o and

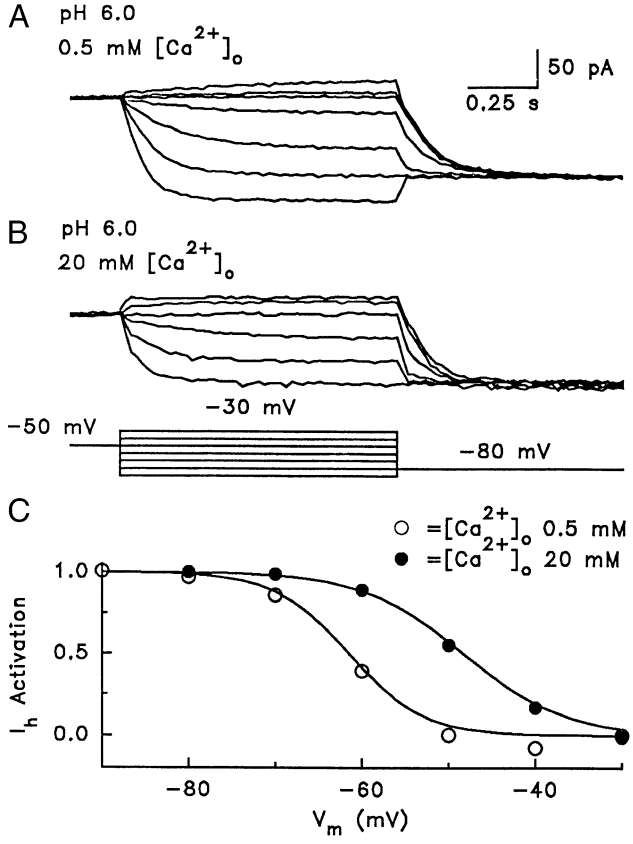

Fig. 7. An acidic environment reduces the effects of Ca^{2+} on gating shifts. (A) Voltage clamp recordings of I_h in $[Ca^{2+}]_o$ of 0.5 and 20 mM while pH_o was 6.0. (B) The activation curves for I_h fitted with Boltzmann function.

Ca^{2+}-induced changes in ψ_o. The predicted shift in I_h activation from the surface potential equations were compared with experimentally derived values including the data in high calcium and low pH.

A model where only screening effects were assumed (Eqs. (2) and (5)) failed to fit the experimental data.

The next model tested assumed that Ca^{2+} and protons bind to common surface charges. This involved solving Eqs. (2) and (5) together with Eq. (3). The following parameters provided the best fit to the experimental data: $\sigma = 1/6.1e^{-}$ $Å^{-2}$, $K_H = 8.1 \times 10^7$ M^{-1} (pK_a 7.91) and $K_{Ca} = 500$ M^{-1}.

To obtain a better fit, Eq. (4), which assumes that protons and Ca^{2+} bind to independent membrane sites, was utilized. This involved solving together Eqs. (2), (4) and (5). The solution that best matched the experimental conditions had the following parameters: $\sigma_1 = 1/33.4e^{-}$ $Å^{-2}$, $\sigma_2 = 1/10.75e^{-}$ $Å^{-2}$, $K_H = 2.0 \times 10^7$ M^{-1} (pK_a 7.29) and $K_{Ca} = 1$ M^{-1}.

4. Discussion

This work examined the effects that pH and Ca^{2+} have on the activation of the hyperpolarization-activated cation current I_h in isolated salamander rod photoreceptors. Our results establish that gating of hyperpolarization-activated I_h in rod photoreceptors is affected in a manner that is essentially identical to that of depolarization-activated ion channels when exposed to surface charge modulating agents such as protons and extracellular calcium. This suggests that the fundamental mechanisms governing the voltage-sensitivity of I_h channel gating are similar to those described for depolarization activated channels. This is consistent with the knowledge that S4 (voltage sensing) regions for both HCN channels and channels activated by depolarization are of similar composition. Classical treatment of I_h kinetics in cone photoreceptors identified at least two 'closed' states, favored by depolarization, and at least three 'open' states, favored by hyperpolarization [5]. Although far from conclusive, our present results support the proposed hypothesis that hyperpolarization-induced transitions from non-conducting to conducting states in HCN channels arise from transitions from inactivated to open states [46]. If so, it seems unlikely that true closed states, favored by strong membrane hyperpolarization, are observed in the HCN channel gating scheme at least over the range of membrane potentials that can be tested.

4.1. Modification of I_h gating by external and internal pH

The changes in gating of HCN channels in salamander rod photoreceptor cells reported here are similar to pH_o-induced shifts that have been observed for other ion channels such as calcium, potassium and calcium-activated chloride channels in photoreceptors, and calcium channels in the heart and sympathetic neurons [6,7,25,28,31,32,33,58]. Quantitatively, the pH_o-induced shifts obtained in this study were similar to the values obtained for rod Kx channels [32] and cardiac Ca channels [31]. Generally, these pH_o-induced shifts in gating have been described by the Gouy–Chapman theory that incorporates alterations to the membrane surface potential caused by proton binding to specific sites on the membrane surface.

However, two recent studies of external pH action on I_h gating found no effects. Heterologously expressed in FLP-IN-293 cells, HCN1 and HCN4 channels showed almost no external pH sensitivity in the range reported in our work, but showed dramatic flattening of the activation curve in the range of pH 3–4 [47]. In rat thalamic slices, no effect of pH_o on I_h whatsoever was detected in experiments with either HEPES or HCO_3^- buffered salines [40].

An earlier study utilizing lobster stretch neurons showed no pH_o-induced shifts in the I_Q activation curve [16]. It was suggested that no shifts were observed because the neurons were exposed to a relatively high (25 mM) $[Ca^{2+}]_o$ which effectively blocked the relatively small changes in the extracellular monovalent concentration.

Whereas the external actions of pH that we described here were apparently not seen in thalamic neurons [40], changing the internal pH of rod photoreceptors altered the gating of I_h in a similar manner as in thalamic neurons. Acidifying the interior of the cell, using sodium acetate, shifted the activation curve to a more hyperpolarized level, similar to the effect seen in thalamic neurons which used lactate or direct acidification of the pipette solution [40]. Alkalinizing the interior, using ammonium chloride, shifted the activation curve to more depolarized potentials, again similar to the thalamic report which used TMA [40]. These shifts were in the opposite direction to the measured extracellular pH induced shifts, which is the expected result because negative charges have been identified on the cytoplasmic membrane surface and the intracellular ionic composition has been shown to alter channel gating [12]. For example, shifts in Na channel gating as $[Ca^{2+}]_i$ was altered that were opposite to the measured shifts induced by extracellular calcium have been reported [13]. This observation was reasoned to be due to alterations in the membrane surface potential. Since our results also show that extracellular and intracellular pH changes shift I_h activation in opposite directions, we propose that intracellular pH alters the cytosolic surface potential.

Assuming that the changes we attempted to make to internal pH were of the same magnitude as the changes measured in rods [44] and horizontal cells [49], then the shifts we observed in $V_{1/2}$ were larger upon changing pH_i than upon changing pH_o. This finding is similar to results obtained with Na channels when intracellular calcium ion concentration was changed [13]. This increase in proton sensitivity might be due to a higher affinity of protons to intracellular sites on the protein (different amino acids are titrated), or to pH effects on channel regulatory mechanisms. A single cytosol-accessible histidine residue has been sug-

gested to determine the pH sensitivity of expressed HCN2 channels, which underlie I_h in heart and brain [59]. Internal pH is known to affect the activity of cAMP-dependent protein kinase (PKA), however, this can be ruled out in the present work since PKA has not been shown to regulate activity of I_h in rods [1,15].

4.2. Modification of I_h gating by Ca^{2+}

I_h activation is altered by changing the external concentration of calcium. This type of alteration of an ion channel by divalent ions has been observed in other ion channels such as Q channels from lobster stretch receptor neurons, Ca channels from heart, K channels from photoreceptors and heart, Na channels from bullfrog skeletal muscle and heart, and h channels from rod photoreceptors [14,16,22,23,26,33,52,53,57]. The divalent-induced shifts in ion channel activation are generally explained on the basis of a surface potential hypothesis. Divalent cations are thought to produce their effect by screening negative surface charges through titration of specific binding sites. Quantitatively, our values are similar to Ca^{2+}-induced shifts previously measured for I_h in rod photoreceptors and I_Q from lobster stretch receptor neurons [16,52].

4.3. Competition between protons and calcium

Our results suggest some degree of interaction between Ca^{2+} and H^+ for membrane surface charges. Interactions between Ca^{2+} and protons have been previously observed: pH- and Ca^{2+}-induced shifts in ion channel gating were reduced as $[Ca^{2+}]_o$ and $[H^+]_o$, respectively, were increased [24,33,42,53].

Although very small shifts remained apparent as a trend, pH_o-induced gating shifts were reduced to a level that did not reach statistical significance when measured in 20 mM $[Ca^{2+}]_o$. This may indicate that protons and Ca^{2+} are competing for the same site, and that at 20 mM $[Ca^{2+}]_o$, most but not all of these sites are occupied by Ca^{2+}. Alternatively, protons and Ca^{2+} may bind to different sites and when Ca^{2+} occupies all of its sites this obstructs protons from reaching their sites.

The persistence of a large Ca^{2+}-induced shift in pH_o 6.0 can be explained by assuming that the proton concentration was not high enough to effectively influence the interaction of Ca^{2+} with the binding sites. This idea seems feasible since it required pH_o 5.0 and lower to neutralize the membrane charges in cardiac ventricular cells [31]. The presence of two binding sites, one where protons and Ca^{2+} ions compete and another where only Ca^{2+} ions bind (see Ref. [33]), is also another possibility.

4.4. Surface potential theory

Divalent and monovalent cation–induced shifts in channel kinetics can be efficiently explained by alterations in the surface potential [16,31]. The surface charge equations that were used in this study were relatively effective in matching the data. Predictions best fit the data when protons and Ca^{2+} were assumed to bind to separate sites; however, the values obtained for surface charge density were not in general agreement with some previously reported results. Our values for charge densities of about one negative charge per few tens of $Å^2$ is much higher than $1/140e^- Å^{-2}$ and $1/300e^- Å^{-2}$ calculated for cardiac cells [23,33] and $1/210e^- Å^{-2}$ calculated for sympathetic neurons [58]. Somewhat different values for pK_a were also observed: Previously published pK_a values ranged from 5.0 to 6.9 [33,58], whereas pK_a 7.29 was calculated using Eqs. (2), (4) and (5) in the present study. This pK_a value suggests that a protein containing an amino acid with an ionizable amino group (pK_a 8.0), e.g. lysine, or sulfhydryl group (pK_a 8.5) may play a role in binding protons. The amino groups of membrane phospholipids could also play a role in attracting protons.

The Ca^{2+}-induced shifts in normal pH (pH 7.6), however, were not adequately fit by assuming H^+ and Ca^{2+} bind to independent or common surface charges. This suggests that Ca^{2+} may have different affinities for the binding sites. For example, at a low $[Ca^{2+}]_o$, Ca^{2+} may bind tenaciously to the channel and eliminate the expected change in surface potential. Another possible explanation is that Ca^{2+} could alter channel function by binding directly to the channel protein and change its conformation in a manner that renders it unable to follow the expected surface potential predictions.

4.5. I_h and the rod response to bright light

Illumination is known to cause changes in pH_o and $[Ca^{2+}]_o$ in the interstitial space surrounding photoreceptor cells. The present results therefore indicate that naturally occurring changes in protons and calcium could modify the rod response to bright light by shifting the voltage range over which I_h activates. Light-induced changes in pH_o have been fairly well characterized as increases in pH of approximately 0.2 pH units in the bulk interstitial space (reviewed in Ref. [4]). Larger alkalinizations may occur in restricted zones around the cells, and in particular, the largest pH changes do occur in the region surrounding the photoreceptor inner segments. A 0.2 pH unit increase would, according to the present assessment, shift the activation of I_h by about 2.5 mV in the negative direction. This in turn would effectively reduce I_h activation, with the net effect on rod membrane potential being a hyperpolarization of about the same magnitude. This could be a significant dynamic modification of the rod bright-light response.

Changes in $[Ca^{2+}]_o$ have also been carefully investigated because such studies held the prospect of defining the role of Ca^{2+} in the phototransduction cascade [56]. Recordings of light-induced increases in $[Ca^{2+}]_o$ appeared to support the original "calcium hypothesis" of phototransduction, yet

were later reinterpreted in view of the still-current perspective that light closes Ca^{2+} permeable channels (the CNG channels of the outer segment) while Ca^{2+} extrusion persists, and that changes in the interstitial volume occur. Nevertheless, light-induced $[Ca^{2+}]_o$ increases of 0.2 to 200 μM remain in the vicinity of the outer segments [21,38,55,56]. At the level of the synaptic terminal and inner segments of rods, where HCN channels are located, the change in $[Ca^{2+}]_o$ appears to be much smaller [17]. Thus it is doubtful that endogenous changes in $[Ca^{2+}]_o$ provide a significant modulating influence on I_h, making $[Ca^{2+}]_o$ an unlikely modifier of the rod light response via this mechanism.

Acknowledgements

The authors are grateful for support from the Canadian Institutes for Health Research (MT-10968 to SB) and the Whitaker Foundation, USA (RG-99-0433 to DEK).

References

[1] A. Akopian, P. Witkovsky, J. Neurophysiol. 76 (1996) 1828–1835.
[2] C.R. Bader, D. Bertrand, E.A. Schwartz, J. Physiol. 331 (1982) 253–284.
[3] S. Barnes, Neuroscience 58 (1994) 447–459.
[4] S. Barnes, in: K. Kaila, B.R. Ransom (Eds.), pH and Brain Function, Wiley, New York, 1998, pp. 491–505.
[5] S. Barnes, B. Hille, J. Gen. Physiol. 94 (1989) 719–743.
[6] S. Barnes, Q. Bui, J. Neurosci. 11 (1991) 4015–4023.
[7] S. Barnes, V. Merchant, F. Mahmud, Proc. Natl. Acad. Sci. U. S. A. 90 (1993) 10081–10085.
[8] D.J. Beech, S. Barnes, Neuron 3 (1989) 573–581.
[9] T. Begenisich, J. Gen. Physiol. 66 (1975) 47–65.
[10] G.A. Borgula, R.H Steinberg, Investig. Ophthamol. Vis. Sci. (Suppl.) 25 (1984) 289.
[11] G.A. Borgula, C.J. Karwoski, R.H. Steinberg, Vis. Res. 29 (1989) 1069–1077.
[12] W.K. Chandler, A.L. Hodgkin, H. Meves, J. Physiol. 180 (1965) 821–836.
[13] S.Z. Cukierman, R.J. French, B.K. Krueger, J. Gen. Physiol. 92 (1988) 431–447.
[14] S. Cukierman, B.K. Krueger, Pflügers Arch. 416 (1990) 360–367.
[15] G.C. Demontis, A. Moroni, B. Gravante, C. Altomare, B. Longoni, L. Cervetto, D. DiFrancesco, J. Physiol. 542 (2002) 89–97.
[16] A. Edman, W. Grampp, Acta Physiol. Scand. 141 (1990) 251–261.
[17] R.P. Gallemore, J.D. Li, V.I. Govardovskii, R.H. Steinberg, Vis. Neurosci. 11 (1994) 753–761.
[18] D.L. Gilbert, G. Ehrenstein, Biophys. J. 9 (1969) 447–463.
[19] R. Gauss, R. Seifert, U.B. Kaupp, Nature 393 (1998) 583–587.
[20] D.C. Grahame, Chem. Rev. 41 (1947) 441–501.
[21] G.H. Gold, J.I. Korenbrot, Proc. Natl. Acad. Sci. U. S. A. 77 (1980) 5557–5561.
[22] R. Hahin, D.T. Campbell, J. Gen. Physiol. 82 (1983) 785–805.
[23] D.A. Hanck, M.F. Sheets, J. Physiol. 454 (1992) 267–298.
[24] B. Hille, A.M. Woodhull, B.I. Shapiro, Philos. Trans. R. Soc. Lond., B 270 (1975) 301–318.
[25] H. Irisawa, R. Sato, Circ. Res. 59 (1986) 348–355.
[26] R.S. Kass, D.S. Krafte, J. Gen. Physiol. 89 (1987) 629–644.
[27] U.B. Kaupp, Annu. Rev. Physiol. 63 (2001) 235–257.
[28] U. Klockner, G. Isenberg, J. Gen. Physiol. 103 (1994) 665–678.
[29] S.J. Korn, A. Marty, J.A. Connor, R. Horn, Methods Neurosci. 4 (1991) 364–373.
[30] P.G. Kostyuk, S.L. Mironov, P.A. Doroshenko, V.N. Ponomarev, J. Membr. Biol. 70 (1982) 171–179.
[31] D.S. Krafte, R.S. Kass, J. Gen. Physiol. 91 (1988) 641–657.
[32] D.E. Kurenny, S. Barnes, Neurosci. Lett. 170 (1994) 225–228.
[33] Y.W. Kwan, R.S. Kass, Biophys. J. 65 (1993) 1188–1195.
[34] C.T. Livsey, B. Huang, J. Xu, C.J. Karwoski, Vis. Res. 30 (1990) 853–861.
[35] A. Ludwig, X. Zong, M. Jeglitsch, F. Hofmann, M. Biel, Nature 393 (1998) 587–591.
[36] S. McLaughlin, Curr. Top. Membr. Trans. 9 (1977) 71–144.
[37] S. McLaughlin, G. Szabo, G. Eisenman, J. Gen. Physiol. 58 (1971) 667–687.
[38] D.L. Miller, J.I. Korenbrot, J. Gen. Physiol. 90 (1987) 397–425.
[39] D.L. Murray, G.T. Feke, J.J. Weiter, Exp. Eye Res. 53 (1991) 717–722.
[40] T. Munsch, H.-C. Pape, J. Physiol. 519 (1999) 493–504.
[41] B. Oakley II, R. Wen, J. Physiol. 419 (1989) 353–378.
[42] H. Ohmori, M. Yoshii, J. Physiol. 267 (1977) 429–463.
[43] M. Piccolino, A.L. Byzov, D.E. Kurennyi, A. Pignatelli, F. Sappia, M. Wilkinson, S. Barnes, Proc. Natl. Acad. Sci. U. S. A. 93 (1995), 2302–2306.
[44] J. Saarikoski, E. Ruusuvuori, A. Koskelainen, K. Donner, J. Physiol. 498 (1997) 61–72.
[45] B. Santoro, D.T. Liu, H. Yao, D. Bartsch, E.R. Kandel, S.A., Siegelbaum, G.B. Tibbs, Cell 93 (1998) 717–729.
[46] B. Santoro, G.B. Tibbs, Ann. N.Y. Acad. Sci. 868 (1999) 741–764.
[47] D.R. Stevens, R. Seifert, B. Bufe, F. Muller, E. Kremmer, R. Gauss, W. Meyerhof, U.B. Kaupp, B. Lindeman, Nature 413 (2001) 631–635.
[48] K.-I. Takahashi, D.R. Copenhagen, J. Neurophysiol. 67 (1992) 1633–1642.
[49] K.-I. Takahashi, D.B. Dixon, D.R. Copenhagen, J. Gen. Physiol. 101 (1993) 695–714.
[50] D.L. Wilson, Y. Morimoto, Y. Tsuda, A.M. Brown, J. Membr. Biol. 72 (1983) 117–130.
[51] L.P. Wollmuth, J. Gen. Physiol. 103 (1994) 45–66.
[52] L.P. Wollmuth, Pflügers Arch. 430 (1995) 34–43.
[53] A.M. Woodhull, B. Hille, Biophys. Soc., Annu. Meet., Abstr. (1970) 111a.
[54] F. Yamamoto, G.A. Borgula, R.H. Steinberg, Exp. Eye Res. 54 (1992) 689–697.
[55] K.-W. Yau, K. Nakatani, Nature 313 (1985) 579–582.
[56] S. Yoshikami, J.S. George, W.A. Hagins, Nature 286 (1980) 395–398.
[57] S. Zalman, I.D. Dukes, M. Morad, Am. J. Physiol. 261 (1991) C310–C318.
[58] W. Zhou, S.W. Jones, Biophys. J. 70 (1996) 1326–1334.
[59] X. Zong, J. Stieber, A. Ludwig, F. Hofman, M. Biel, J. Biol. Chem. 276 (2001) 6313–6319.